

# ***Quantifying weak interactions between iodide and clay minerals***

**Fuel Cycle Research & Development**

*Prepared for  
U.S. Department of Energy  
Used Fuel Disposition Program  
Andrew Miller, Yifeng Wang,  
Jessica Kruichak, Melissa Mills,  
Hernesto Tellez  
Sandia National Laboratories  
May 21, 2012  
FCRD-UFD-2012-000121*



**DISCLAIMER**

This information was prepared as an account of work sponsored by an agency of the U.S. Government. Neither the U.S. Government nor any agency thereof, nor any of their employees, makes any warranty, expressed or implied, or assumes any legal liability or responsibility for the accuracy, completeness, or usefulness, of any information, apparatus, product, or process disclosed, or represents that its use would not infringe privately owned rights. References herein to any specific commercial product, process, or service by trade name, trade mark, manufacturer, or otherwise, does not necessarily constitute or imply its endorsement, recommendation, or favoring by the U.S. Government or any agency thereof. The views and opinions of authors expressed herein do not necessarily state or reflect those of the U.S. Government or any agency thereof.

# FCT Quality Assurance Program Document

## FCT Document Cover Sheet

Name/Title of Deliverable/Milestone Radionuclide interaction with clays and colloids  
 Work Package Title and Number Natural Systems Evaluation-SNL FT-12SN080708  
1.02.08.07 Milestone Number M3FT-12SN0807087  
 Work Package WBS Number \_\_\_\_\_  
 Responsible Work Package Manager Yifeng Wang 5-8-12  
 (Name/Signature) (Date Submitted)

Quality Rigor Level for Deliverable/Milestone	<input type="checkbox"/> QRL-3	<input type="checkbox"/> QRL-2	<input type="checkbox"/> QRL-1 <input type="checkbox"/> Nuclear Data	<input checked="" type="checkbox"/> N/A*
---	--------------------------------	--------------------------------	---	--

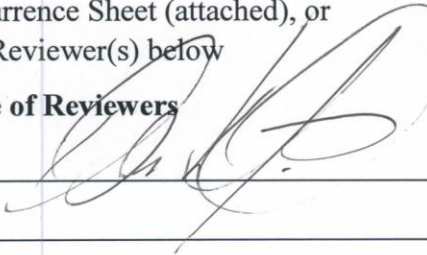
This deliverable was prepared in accordance with Sandia National Laboratory  
 (Participant/National Laboratory Name)

QA program which meets the requirements of  
 DOE Order 414.1     NQA-1-2000     Other: \_\_\_\_\_

**This Deliverable was subjected to:**

- |   |   |
|---|---|
| <input checked="" type="checkbox"/> Technical Review                  | <input type="checkbox"/> Peer Review                                  |
| <b>Technical Review (TR)</b>  | <b>Peer Review (PR)</b>   |
| <b>Review Documentation Provided</b>                                  | <b>Review Documentation Provided</b>                                  |
| <input type="checkbox"/> Signed TR Report, or<br>TR Report No.: _____ | <input type="checkbox"/> Signed PR Report, or<br>PR Report No.: _____ |
| <input type="checkbox"/> Signed TR Concurrence Sheet (attached), or   | <input type="checkbox"/> Signed PR Concurrence Sheet (attached), or   |
| <input checked="" type="checkbox"/> Signature of TR Reviewer(s) below | <input type="checkbox"/> Signature of PR Reviewers below              |

**Name and Signature of Reviewers**

Carlos Jove-Colon/  5-9-2012  
 \_\_\_\_\_  
 (Name/Signature) (Date)

\*Note: In some cases there may be a milestone where an item is being fabricated, maintenance is being performed on a facility, or a document is being issued through a formal document control process where it specifically calls out a formal review of the document. In these cases, documentation (e.g., inspection report, maintenance request, work planning package documentation, or the documented review of the issued document through the document control process) of the completion of the activity along with the Document Cover Sheet is sufficient to demonstrate achieving the milestone. QRL for such milestones may also be marked N/A in the work package provided the work package clearly specifies the requirement to use the Document Cover Sheet and provide supporting documentation.

## INTRODUCTION

Clays will play an important role in nuclear waste isolation. Besides being ubiquitous in natural systems, clay minerals may also be used as backfill or sealant material and may be the host rock surrounding the engineered disposal gallery. The major advantages of clays are their low permeability and high sorption capacities. Much of the sorption capacity stems from the fixed negative charge present on the basal surface of clay minerals. This negatively charged surface presents a large number of sorption sites for cations but repels anions. The repellent behavior has led to treating anions as non-reactive and thus highly mobile in the performance assessment of nuclear waste repositories. This assumption translates into anions being the largest dose contributors at times >10,000 years for clay based repositories. However, literature data shows that many anions, including iodine, are retarded in clays relative to tritiated water. Tritiated water is assumed to act similarly to pore water and is the ultimate non-reactive tracer. It is assumed that the anion retardation occurs due to sorption, which is often quantified with a  $K_D$  value. These values are small; iodide  $K_D$  values have been reported from ~0.001-2.9mL/g. While small, the assumption that the iodide will behave conservatively overestimates iodine dose in performance assessment analysis. Furthermore, constraining the mechanism of iodine uptake to clays may allow for material development with much larger retardation of iodine. Currently, little headway has been made with respect to understanding how a negatively charged ion interacts with a negatively charged surface.

Understanding iodine interactions with clays is hampered by two main complicating factors. First, since the total amount of interaction is relatively low, it is hard to reliably detect. To circumvent this issue high solid:solution ratios are typically used in batch experiments and radiotracers are used to improve detection limits. The use of radiotracers is the second complicating factor, as the oxidation state of iodine in radiotracers is not always known. Recent experimentation has shown that the oxidation state in radio-iodine stocks can be mixed (typically iodide (-1) and iodate (+5) are present), and that the observed iodine interactions with clays depends strongly on the redox state of iodine. Gamma detection for radioiodine cannot distinguish oxidation state. Because of these two experimental issues, literature interpretations of iodine interactions with clays are often contradictory. In diffusive columns, iodide, when purposefully separated from iodate, has been shown to act similarly to chloride. In other diffusive systems, unpurified radioiodine appears to be retarded relative to chloride. Iodine oxidation state has also been shown to change upon contact with clay minerals. Because of the conflicting information and experimental artifacts, delineating uptake mechanisms from available data is difficult.

A final issue with available data is that iodine uptake studies, batch or diffusive columns, most often use a single clay mineral. Because they are the target minerals for backfill or host rock for certain international waste programs, most nuclear waste related experiments to date include only illite and montmorillonite. A few also include kaolinite as a 'simpler' analogue. From an experimental perspective this is advantageous as it simplifies the amount of clay purifications that are necessary. It also follows the traditional aspect of sorption studies used to examine ion exchange and surface complexation reactions. However, the use of a single clay forces interpretation of uptake within the confines of classical clay surface chemistry. It removes the ability to compare uptake as a function of other known clay characteristics, including: fixed charge, distinguishing contributions of fixed from amphoteric charge contributions, structural characteristics of clay minerals, and variable pore scale chemistry caused by constrained space within the clay mineral.

In this study, iodide uptake experiments to seven different clay minerals are completed. Each of these minerals is characterized using BET surface area. Edge protonation state distributions are studied on all seven clay minerals through surface titrations and fixed charge is characterized by cation exchange capacity (CEC) determinations. Iodide uptake was determined through batch experimentation using a

wide range of swamping symmetric electrolyte identity and concentrations. Iodide uptake is clearly linked to cation exchange capacity. It appears that the iodide is concentrating in the interlayer spaces of the clays, which is specifically contraindicated from classical clay surface chemistry. Contrary to literature discussion, the data collected here is pointing to an uptake mechanism that is not based on a traditional surface interaction (i.e., ion exchange and surface complexation). Instead, iodide uptake appears to be related to the amount of fixed surface charge and to the physical structure of the clay. Uptake is inferred to occur due to the unique nano-environments formed from the combination of fixed charge and structurally constrained space.

## **EXPERIMENTAL METHODS**

### **Clay minerals and purification**

The clays used all originate from the Clay Mineral Society source clays project at Purdue University. Seven total clays were used including: kaolinite, ripidolite, illite, montmorillonite, palygorskite, sepiolite, and a 70/30 illite/smectite mixed layer (ID numbers: KGa-1b, CCa-2, IMt-1, SWy-2, PFI-1, SepNev-1, and ISCz-1, respectively). The clays used were relatively pure; however, for several of the clays purification steps were required to remove certain impurities. The main purification step used for all of the clays was mechanical separation at 75 microns. The <75 microns size fraction was used in all the experiments presented here. Each clay was examined by XRD for impurities. The kaolinite, sepiolite, and ripidolite did not have any measurable impurity minerals. All of the other clays had measurable amounts of quartz. There were no other clearly identifiable oxides or carbonates. The best match to the illite spectra was muscovite, although due to the small degree of crystallinity, the spectra peaks were small. The XRD spectra for the illite/smectite mixed layer clay most closely resembled pure illite, although the match was not exact.

In initial titration experiments, described below, the illite and montmorillonite samples showed significant buffer capacity around pH 8.3. It was assumed that this was a calcite impurity, as the initial titration curves were significantly different from other published sources. To remove the calcite, these two clays were washed and converted to the sodium form with ion exchange and centrifugation. Both clays were mixed with a 0.1M NaCl solution overnight. For illite, a single centrifugation for 60 minutes at 4400g was sufficient to pelletize the clay. The montmorillonite often required several centrifuge cycles (6-7 hours). Once a pellet was formed, the solution was decanted and discarded, and fresh NaCl solution was added. The mixing and centrifugation processes were repeated. The entire process was repeated two more times with DI water. Once the clays were washed they were dried in a 100°C oven for several days. This exchange method was also used to convert the clays for CEC determinations described below.

### **Titration experiments**

The surface titration of the clays was completed with a Mettler Toledo DL55. For each analysis 1g of clay mineral was added to 50mls of the swamping electrolyte. Electrolytes used were 0.01, 0.1, and 0.5M NaCl solutions. The solution was constantly sparged with nitrogen to exclude atmospheric carbon dioxide. Upon addition of the clay, the solution was stirred and sparged until the pH stabilized. This generally took 10-30 minutes. Titrations were separated at the natural pH of the clay in the electrolyte.

For each ionic strength, one clay sample was titrated up to pH 10.5 (base leg) while a separate sample was titrated down to pH 2.5 (acid leg). The titrants were 0.1M HCl or 0.1M NaOH. The NaOH solution was always made immediately before use to minimize CO<sub>2</sub> dissolution. The titrants were added in 0.1mL increments. Between additions, the rate of pH change was <0.02 pH unit/second for seven seconds. The results from the two legs were combined to create the entire titration curve. Blank titrations and titrations of a commercial AlO powder were also completed. Because of the smaller surface area of the AlO powder, 5 grams of material had to be used instead of 1g. The longest titrations required about 20 hours to complete, while the shortest required only 10-20 minutes. The titrations were completed in triplicate, and the averaged response is shown below.

### CEC determination

The method used follows that of [1]. This method requires that the clays be in the sodium exchanged form. This was completed for all of the clays through ion exchange and centrifugation described above. To determine CEC, an increasing ratio of methylene blue to clay was added. For all of the clays except montmorillonite, this was completed by adding a fixed mass of clay (0.2g) and variable concentrations of methylene blue (up to 1E-2 M). For montmorillonite, the large CEC value required smaller masses of clay (down to 0.02g) to increase the ratio of methylene blue to clay. Initial experimentation showed minimal methylene blue wall sorption in the 15mL centrifuge tubes used for the reaction. The clay/methylene blue mixture was mixed for 4 hours. At the end of four hours the suspension was centrifuged at 2600g until a sample could be removed from the supernatant. This required between 1-4 hours depending on the clay. Methylene blue was quantified using a spectrophotometer at 670nm. Sorption isotherms were created plotting the amount of methylene blue sorbed vs. the amount added. Deviation from a 1:1 line demarcated the endpoint, and the CEC was interpolated from the plot. An example figure is shown for ripidolite in Figure 1.

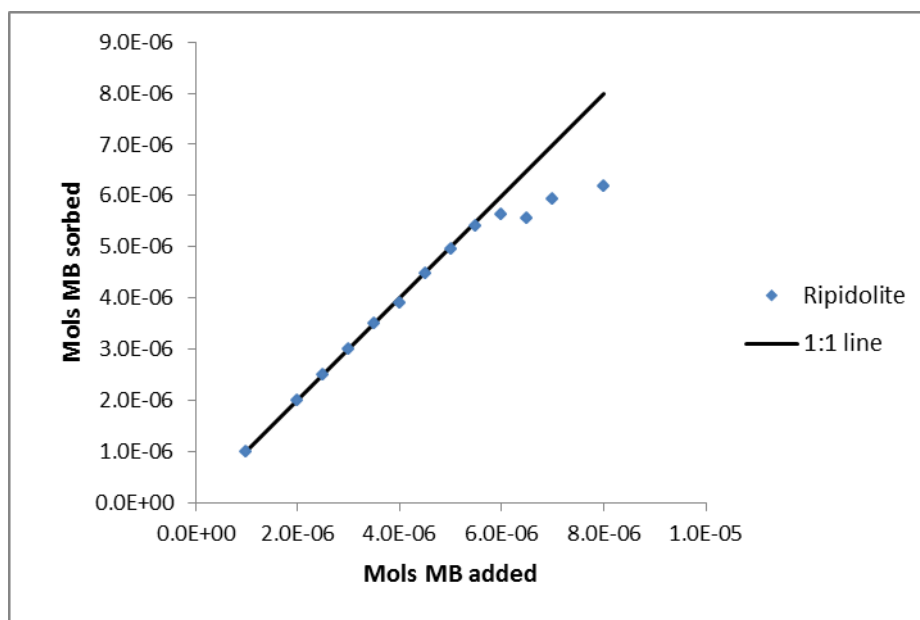


Figure 1- Mols methylene blue sorbed vs. mols added for ripidolite.

## Iodide sorption experiments

Batch iodide sorption experiments were completed in triplicate for all of the clay minerals. The only purification step performed on the clays was dry-sieving at 75 microns. The <75 micron fraction was used. A constant iodide concentration of 3.94E-4 M (50mg/L) was used for all of the batch reactors. For each set of experiments, the ionic composition and concentration of the swamping electrolyte was held constant. The electrolytes and concentrations used are shown in Table 1. A constant solid:solution ratio of 100g/L was used in all of the experiments.

**Table 1-** Experimental summary of electrolytes and concentrations. An X denotes which were used in these experiments.

Concentration (M)	NaCl	NaBr	KCl
1.0	X		
0.1	X	X	X
0.01	X		

The batch reactors were 50mL centrifuge tubes. Blanks confirmed the absence of wall sorption or iodide loss to volatilization. To each tube the clay and electrolyte solution was added, and the suspensions were equilibrated overnight. An iodide spike was added after equilibration. The spike was an ion chromatography (IC) iodide standard with no detectable iodate. The batch reactors were mixed in the dark at room temperature for 7 days in a horizontal position on a shaker table. After 7 days, the samples were centrifuged for 1 hour at 4400g. The supernatant was removed with a pipette and refrigerated for analysis. The pH was measured immediately before the iodide spike was added, and again at the end of the 7 day mixing period both before and after centrifuging. No attempt was made to keep the pH constant or at a specific level. The pH reported is the equilibrium pH for the given clay minerals in the specified electrolyte. After the uptake sample had been removed, an equal amount of DI water was added to the vial. The slurry was mixed for four days. At the end of four days the sample was centrifuged as above, and a sample was removed for analysis. This sample represents a reversal of the uptake process, and gives information regarding the oxidation state of the iodine species after uptake.

The samples were analyzed using a Dionex 1100 ion chromatograph (IC) with an AS23 guard and analytical column, and a bicarbonate/carbonate eluent. Methods were developed to simultaneously measure iodide and iodate.

## RESULTS

### pK<sub>a</sub> distributions

Surface charge of clay minerals ( $\sigma_0$ ) can be calculated from the titration curves using equation 1[2],

$$\sigma_0 = \frac{(C_A - C_B + [OH^-] - [H^+])F}{S_a} \quad (\text{Eq. 1})$$

where  $C_A$  and  $C_B$  are the concentrations of acid and base needed to attain a specific pH on the titration curve,  $[OH^-]$  and  $[H^+]$  are the  $OH^-$  and  $H^+$  concentrations,  $F$  is the Faraday constant (96,490 C/mol) and  $S_a$  is the surface area of the clay mineral. In performing these calculations, the measured BET surface area was used. In the case of clays, this method does not give total surface charge as it does not take into account the fixed charge of the clay surfaces. More accurately, this method quantifies the total amount of proton sorption to the clay, and converts this to sorbed proton charge. Assuming that the protons exhibit Langmuirian behavior, the protonation state of clays ( $Q$ ) can be calculated and related to the binding site distribution ( $f(pK)$ ), and the acidity constants ( $pK$ ) by equation 2,

$$Q = \int_{pK_{min}}^{pK_{max}} \frac{f(pK)}{1 + 10^{-pK+pH}} d(pK) \quad (\text{Eq. 2})$$

$Q$  is calculated from the titration curves, and the distribution of acidity constants is calculated from deconvolution of Eq. 2 with the condensation approximation (equation 3),

$$f(pK) \approx \frac{dQ}{dpH} \quad (\text{Eq. 3})$$

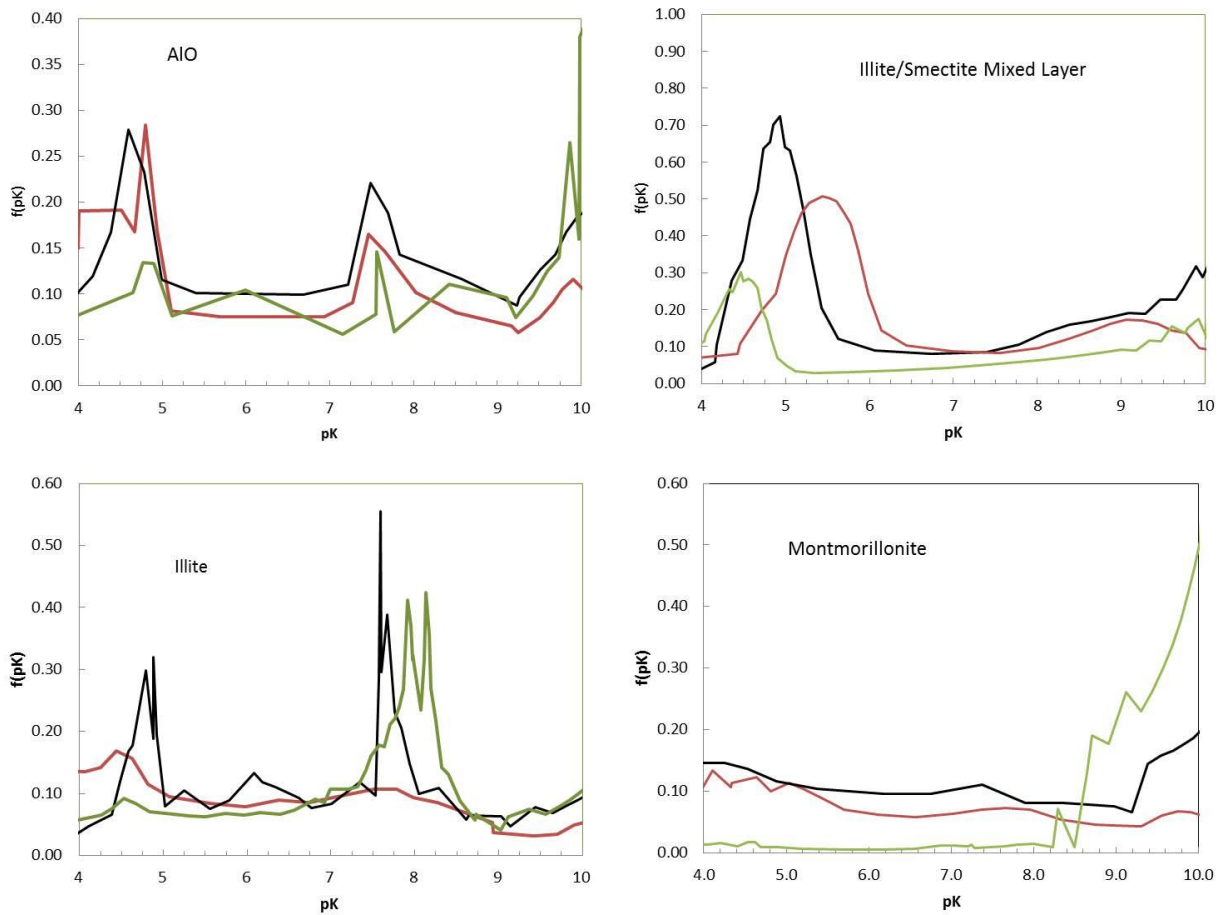
The calculated distribution of sites is presented using a five-point smoothing window. The individual distributions are shown in Figures 2 and 3.

For many of the clays and for the AIO material, the behavior of the  $pK$  distributions was erratic at  $pH < 4$  and  $> 10$ . It is suspected that dissolution of the minerals was occurring which interferes with the titration process. The results and discussion here are restricted to  $pH$  values between 4 and 10. The  $pK$  values are read directly from the plots;  $pK$  values correspond to the peaks in the curves. For example, the AIO plot has two distinct peaks at  $pH$  4.7 and 7.5 for both 0.01M and 0.1M NaCl concentrations. When the ionic strength is at 0.5M, other peaks may be present. A major point from these curves, which is elaborated below, is that for changing ionic strengths, the AIO peaks are largely invariant. For nearly all of the clay minerals, there are significant changes as a function of ionic strength. For some clays it appears that the increase in ionic strength diminishes surface proton activity by suppressing the peaks (e.g., ripidolite). In others it appears that more peaks are present with increasing ionic strength (e.g., palygorskite). And in others the number of peaks is similar but the  $pK$  value is shifted (e.g., illite/smectite mixed layer).

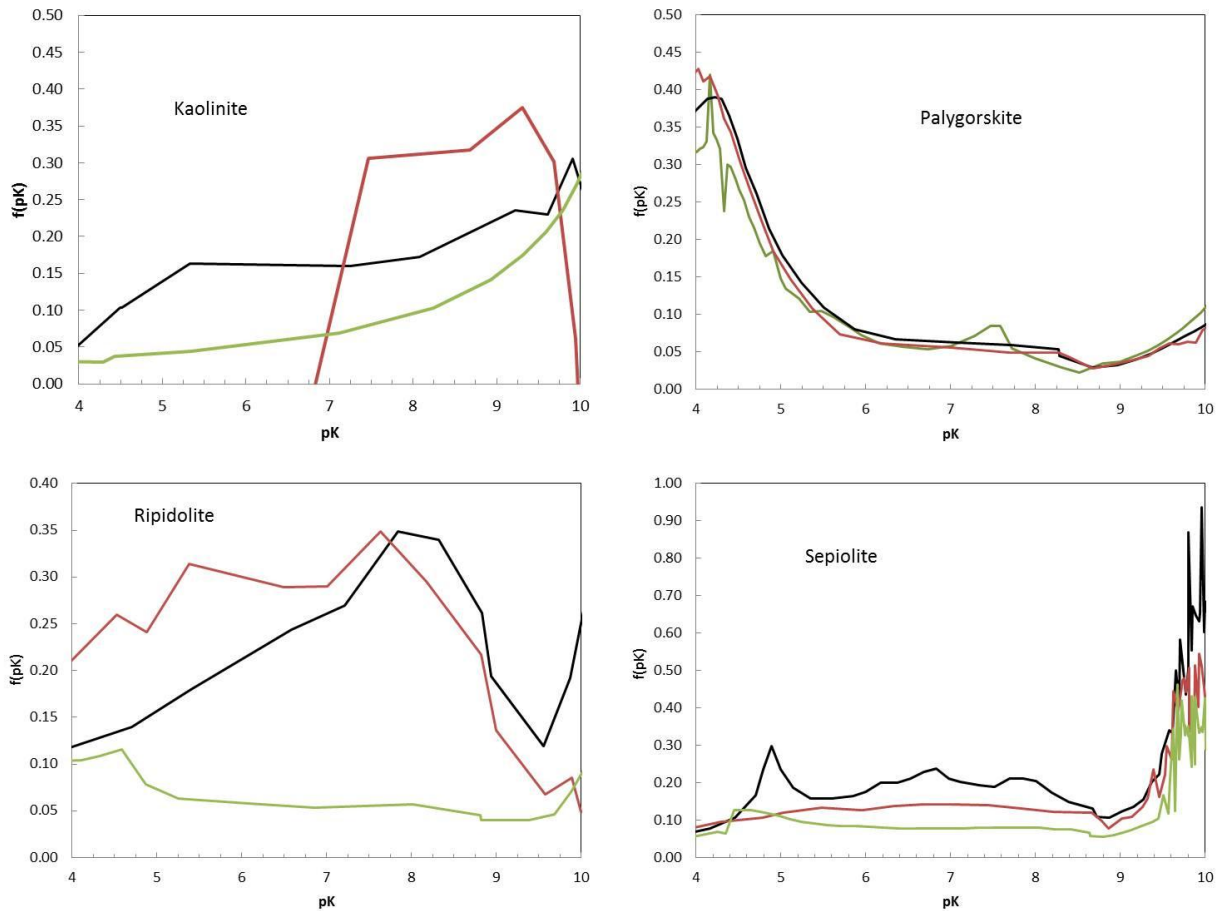
### CEC and surface area

Table 2 shows the results of the methylene blue experiments. Besides direct determination of CEC, methylene blue also allows for the calculation of surface area assuming monolayer sorption and a molecular area of  $130 \text{ \AA}^2$ . Generally methylene blue surface areas are higher than BET surface area determinations. Also the discrepancy increases as the CEC increases. The classical interpretation is that the BET surface area represents only the 'external' surface area of a clay; the interlayer space is inaccessible to the nitrogen molecules. Because the methylene blue determinations take place in aqueous suspension, it is assumed that the clays can delaminate, and the methylene blue surface area is more representative of the 'total' surface area of a clay. The difference between them is the interlayer area. All of these surface areas are reported in Table 2. Sepiolite is the one exception to the general behavior. The BET surface area was larger than the methylene blue surface area. This leads to the physically meaningless negative internal surface area shown in Table 2.





**Figure 2** pK<sub>a</sub> distributions for AIO, illite, illite/smectite mixed layer, and montmorillonite. The red, black and green lines represent 0.01M, 0.1M, and 0.5M NaCl, respectively.



**Figure 3** pK<sub>a</sub> distributions for kaolinite, ripidolite, palygorskite, and sepiolite. The red, black and green lines represent 0.01, 0.1 and 0.5M NaCl concentrations, respectively.

**Table 2-** CEC and surface area values for the clays used. Surface area determination methods are explained in the text.

	CEC (meq/100g)	BET S.A. (m <sup>2</sup> /g)	Total S.A. (m <sup>2</sup> /g)	Internal S.A. (m <sup>2</sup> /g)
Kaolinite	1.50	11.31	11.76	0.45
Ripidolite	3.00	8.02	23.49	15.47
Illite	14.98	31.46	117.21	85.76
Illite/Smectite	24.69	29.82	193.23	163.41
Montmorillonite	109.53	28.29	857.17	828.88
Sepiolite	17.41	201.43	136.27	-65.16
Palygorskite	39.96	141.52	625.45	483.93

## Iodide batch uptake experiments

Tables 3 and 4 show the pH values at the different points in the experiments. Table 3 shows the pH values for equimolar electrolyte concentrations but varying electrolyte identities. Table 4 shows the pH values for varying concentrations of NaCl electrolytes. In general the values are somewhat bimodal being centered around pH 4 or pH 8. During the course of mixing, the pH changed only slightly, typically decreasing within  $\sim 0.2$  pH units. Centrifuging caused larger shifts in pH, the largest being 0.98 pH units for the KCl electrolyte experiments with ripidolite. Differences between equimolar electrolytes are fairly small suggesting similar  $\text{Na}^+/\text{H}^+$  and  $\text{K}^+/\text{H}^+$  exchange constants. With increasing sodium concentration, the pH decreases consistent with  $\text{Na}^+$  exchange for  $\text{H}^+$  on the basal surfaces of the clays.

Because solid:solution ratio and added iodide were consistent across the experiments, the removals are shown as a percent in Tables 5 and 6. Table 5 shows the percent removal as a function of electrolyte, Table 6 shows the percent removal as a function of NaCl concentration. Negative values are most likely caused by anion exclusion due to the fixed negative charge of the clay interface. Generally removals decrease as a function of increasing CEC. However, palygorskite and sepiolite act significantly different than the other clays, this is discussed in detail below. For equimolar concentrations, NaCl has the highest removals, followed by NaBr then KCl. The relative standard deviations were generally quite good. IC instrumental variation alone has been estimated at about 2%. For several of the more egregious RSD values, more replicates are currently being performed.

For experiments where the electrolyte identity was held constant and the concentration was variable, the iodide uptake behavior separates into two classes. Iodide uptake peaked at 0.1M NaCl concentrations for kaolinite, ripidolite, illite, illite/smectite, and sepiolite. Removals got progressively larger with increasing electrolyte concentration for montmorillonite and palygorskite.

**Table 3-** pH values at different points in the experiment for equimolar electrolytes

	0.1M Electrolyte								
	NaCl			NaBr			KCl		
	Before spike	Before Centrifuging	After Centrifuging	Before spike	Before Centrifuging	After Centrifuging	Before spike	Before Centrifuging	After Centrifuging
Kaolinite	4.23	4.21	4.39	4.43	4.47	4.28	4.18	4.12	4.07
Ripidolite	8.73	8.51	8.10	8.76	8.63	8.20	8.79	8.59	7.81
Illite	8.45	8.27	8.16	8.48	8.31	7.95	8.28	8.08	8.01
Illite/Smectite	4.00	4.06	4.24	4.22	4.26	4.03	3.91	3.85	3.82
Montmorillonite	8.15	8.05	8.05	8.19	8.14	8.05	8.09	8.03	7.90
Sepiolite	7.89	7.66	7.83	7.98	7.63	7.75	7.92	7.64	7.80
Palygorskite	7.98	7.76	7.90	8.05	7.84	7.82	7.84	7.63	7.87

**Table 4-** pH values at different points in the experiment for changing concentrations of NaCl electrolyte

	NaCl Electrolyte								
	0.01M			0.1M			1.0M		
	Before spike	Before Centrifuging	After Centrifuging	Before spike	Before Centrifuging	After Centrifuging	Before spike	Before Centrifuging	After Centrifuging
Kaolinite	4.70	4.83	4.73	4.23	4.21	4.39	4.04	4.27	4.19
Ripidolite	8.79	8.57	8.15	8.73	8.51	8.10	8.74	8.59	8.37
Illite	8.68	8.46	8.30	8.45	8.27	8.16	8.37	8.22	7.87
Illite/Smectite	4.38	4.57	4.40	4.00	4.06	4.24	3.57	3.65	3.74
Montmorillonite	8.65	8.55	8.50	8.15	8.05	8.05	7.78	7.77	7.73
Sepiolite	7.92	7.64	7.83	7.89	7.66	7.83	7.78	7.50	7.71
Palygorskite	8.17	7.93	7.99	7.98	7.76	7.90	7.83	7.75	7.75

**Table 5-** Percent removal and percent relative standard deviation for iodide removal in 0.1M electrolytes.

	CEC	% removal			% RSD		
	meq/100g	NaCl	NaBr	KCl	NaCl	NaBr	KCl
Kaolinite	1.50	13.8	3.7	-0.1	2.4	6.5	2.2
Ripidolite	3.00	10.1	2.4	-3.2	3.4	7.6	1.8
Illite	14.98	4.6	1.3	-5.3	5.9	0.0	2.5
Illite.Smectite	24.69	3.6	-0.1	-5.1	0.7	1.1	1.1
Montmorillonite	109.53	-3.4	-6.1	-21.4	3.5	0.7	11.4
Sepiolite	17.41	0.1	7.3	1.0	2.8	1.3	2.9
Palygorskite	39.96	2.3	11.2	9.0	3.0	0.5	1.6

**Table 6-** Percent removals and percent relative standard deviation for iodide removal in varying concentrations of NaCl electrolyte.

	CEC	% removal			% RSD		
	meq/100g	0.01M	0.1M	1.0M	0.01M	0.1M	1.0M
Kaolinite	1.50	4.5	13.8	1.0	2.5	2.4	2.9
Ripidolite	3.00	1.3	10.1	4.2	2.1	3.4	1.6
Illite	14.98	-4.9	4.6	2.6	4.4	5.9	2.1
Illite.Smectite	24.69	-1.6	3.6	2.9	2.6	0.7	0.8
Montmorillonite	109.53	-15.9	-3.4	5.7	6.2	3.5	0.8
Sepiolite	17.41	5.6	0.1	-0.2	29.5	2.8	3.1
Palygorskite	39.96	-2.6	2.3	6.5	5.4	3.0	2.4

## DISCUSSION

### Titration

Aluminum oxide acts as a simple model system in this series of experiments; it both confirms the methodological process and acts as a frame of reference for understanding the clay behaviors. As expected from surface complexation theory as well as other experiments and models, the  $pK_a$  values are largely invariant as a function of ionic strength. Small shifts may be attributable to changes in chemical potential as a function of ionic strength. This effect is not taken into account with the titration curve inversion method. It does appear that there may be other peaks starting to appear at the highest ionic strength studied, although there is no ready explanation for this behavior.

The clays have a much broader range of behaviors (Figures 2 and 3). Illite, illite/smectite mixed layer, and montmorillonite set up a continuum of minerals (smectite and montmorillonite are synonymous in this case). These three clays represent two mineral endmembers with an intermediate of mixed composition. The major  $pK_a$  values for illite are centered at a pH of about 8 with smaller peaks at pH  $\sim$ 4.6. There also appears to be more  $pK_a$  peaks at 0.1M NaCl than at either 0.5 or 0.01M NaCl. The illite/smectite mixed layer has some of the most consistent behavior across the range of ionic strength. The major  $pK_a$  peak is ionic strength dependent. At low ionic strength it is centered at pH 5.5, at 0.1M ionic strength the peak is centered at pH 5, and at the highest ionic strength the peak is centered at pH 4.5. This peak shifting is far more extreme than was seen for the AIO material, so it can be surmised that the shift is caused by something other than changing EDL potential. Since the change in ionic strength corresponds with a change in the sodium concentration, this shift may be representative of the  $Na^+/H^+$  exchange reaction. If this is the case, it is unclear why a similar reaction was not seen in the montmorillonite sample where  $Na^+/H^+$  exchange would also be common. For montmorillonite the  $pK_a$  distribution is not particularly remarkable. The surface appears proton neutral independent of ionic strength. At the highest ionic strength there appears to be a broad peak starting at pH 8 which does not return to 'baseline' in the experimental range; this may be attributable to the same mechanisms which cause similar noise at pH  $>10$ . Despite the continuum of mineralogy, there is no consistency between the  $pK_a$  distributions of these three minerals. From the observable scale, the clay minerals seem to act independently; the illite/smectite behavior is not dominated by the contribution of either of the endmembers.

Kaolinite is proton neutral at both 0.5M and 0.1M NaCl values. At the 0.01M NaCl values, there is a broad peak ranging from pH 7 to 10. Ripidolite becomes progressively more proton neutral with increasing ionic strength. At the lowest ionic strength there are three potential peaks. At the intermediate ionic strength there is a single broad peak centered at pH 8.2, while at the highest ionic strength there is only a single discernible peak at pH 4.5. This type of behavior is consistent with a 'masking' of surface effects as a function of increasing ionic strength. The increased sodium may be dampening the effect of proton sorption.

Sepiolite and palygorskite are structurally similar minerals. Both are fibrous in nature but have differently sized pore spaces which allow for different amounts of associated water. They are also chemically distinct as palygorskite has structural aluminum, and sepiolite is a pure magnesium silicate. Unsurprisingly their titration data is also quite distinct. Sepiolite appears proton neutral, except for a peak at pH 5 at 0.1M ionic strength. The noise at pH  $>9.5$  continues as pH increases, and this is attributed to dissolution. Palygorskite has similar behaviors independent of ionic strength. There is a large single peak at 4.2, and a smaller peak at pH 7.5 when ionic strength is 0.5M. The  $pK_a$  values of palygorskite are similar to those of the pure AIO. This was the anticipated result from all of the clays

expect for sepiolite. All of the other clay minerals used have edge aluminol sites that may have similar behavior to the surface sites of AlO. The lack of  $pK_a$  peaks for the clay minerals either means that the overall differences between AlO and clay alters the acidity of the edge aluminol sites so that they are no longer comparable [3], or some other process besides surface protonation is dominating behavior (i.e.,  $Na^+/H^+$  exchange).

### CEC and iodide uptake

The advantage of the experimental setup is comparisons can be made between uptake and fundamental clay structures. Clays are layered alumino-silicates with discrete tetrahedral (Si-O) and octahedral (Al-O or Mg-O) layers. The physical layering and specific chemical identities within these layers and the smallest repeating unit of the clay layers all dictate clay mineral identity. The smallest repeating unit for kaolinite is two layers, one being tetrahedral, one being octahedral (1:1 clay). For illite, illite/smectite, and montmorillonite the smallest repeating unit is an octahedral layer sandwiched between two tetrahedral layers (2:1 clay). Ripidolite is also a 2:1 clay, but the smallest repeating unit has an extra octahedral layer present between the 2:1 layering. All of these clays are layered clays, and can be physically represented at a larger scale by a stack of plates, where the interlayer space is the plane between the plates. Sepiolite and palygorskite are both fibrous clays. They both have a 2:1 repeating unit, but the individual plates invert in a regular pattern. Thus the interlayer space is long and columnar instead of being planar as in the layered clays. The void in palygorskite is slightly smaller than that of sepiolite. Using these physical descriptions, it is clear the fibrous clays are behaving quite differently from the layered clays. In Table 5 the behaviors of the layered clays are inverted relative to the fibrous clays. When conditions allowed for large uptake in the layered clays, uptake was low in the fibrous clays. When uptake was small in the layered clays, it was larger in the fibrous clays. When NaCl was used uptake in the fibrous clays was small independent of concentration. The differences between the clays imply an uptake mechanism dependent on the size and shape of the interlayer space.

To help develop a physical conceptual model of iodide interaction with the clay minerals, the molar uptake was normalized to the three different surface areas and plotted as a function of CEC (Figures 4-6). The figures shown are from the 0.1M NaCl experiments. Uptake can be expressed through equation 4:



where  $\equiv X$  represents an exchange site on the clay surface, and  $\equiv XI^-$  represents iodide that has been taken up by the clay surface. While this equation is identical in form to that typically used for cation exchange on clays, the use here is not intended to imply a mechanism. The  $\equiv X$  site is more broadly representative of an unknown, but surface based interaction between iodide and the clay. Using this reaction as a guide to Figures 1-3, the CEC is analogous to  $\equiv X$  (x-axis) and the iodine surface concentration is represented by the  $\equiv XI^-$  (y-axis). Using the equation above, a linear log-log plot of surface concentration to CEC would be expected. When normalized to BET (external) surface area, this is not the case. When normalized to the methylene blue (total) or internal surface area the plots become more linear. Negative uptakes or surface area (internal sepiolite) do not plot in log-log space. The linear relationship implies an uptake mechanism associated with the total or interior surfaces of the clay, as opposed to the external surfaces of the clay. It also minimizes the possibility that the iodide is interacting with the edge sites through a traditional surface complexation formation mechanism. If that

had been the case, the linear relationship would have been strongest when normalized to the BET surface area.

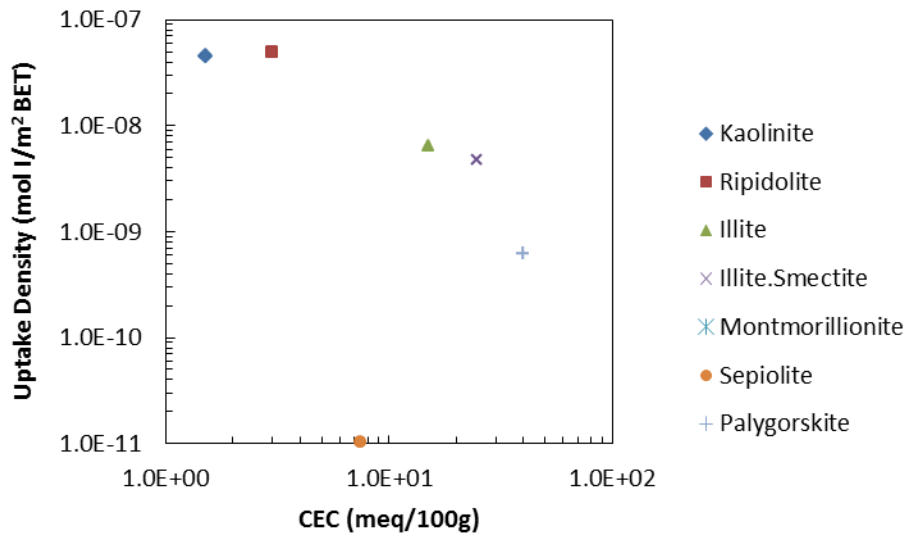


**Figure 4-** Uptake density normalized to BET surface area vs. CEC. The error bars represent plus/minus one relative standard deviation.

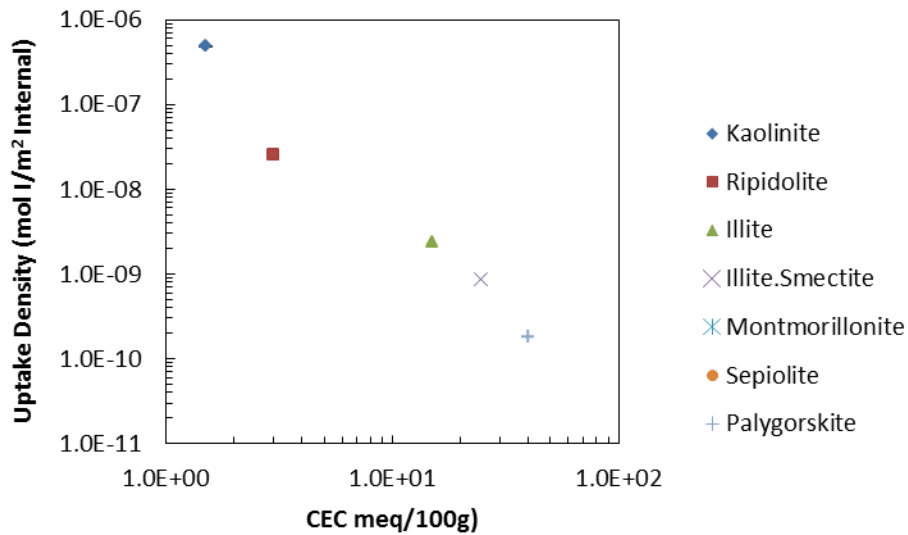


**Figure 5-** Uptake density normalized to internal surface area vs. CEC. The error bars represent plus/minus one relative standard deviation.



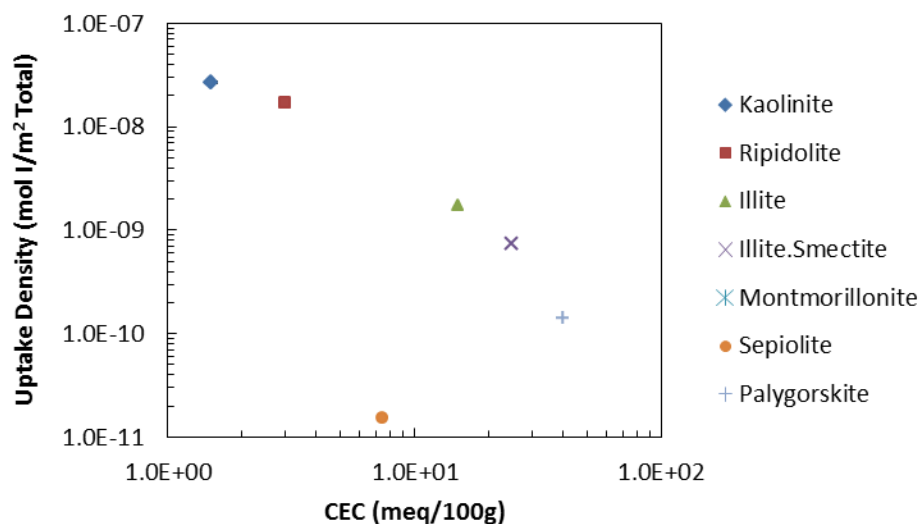


**Figure 6-** Uptake density normalized to total surface area vs. CEC. The error bars represent plus/minus one relative standard deviation.

The interaction of iodide in the interlayer spaces is problematic if using the classical surface chemical interpretation of a clay surface. Using a classical interpretation, the data implies that negatively charged iodide is concentrating at the very surface where the fixed negative charge is located. Charge repulsion constraints dictate that this should not occur. When considering only the percent removals, the charge repulsion arguments would seem to hold. Smaller CEC values (smaller fixed negative charge) have larger amounts of uptake. However, the surface charge characteristics should be identical for equimolar NaCl and NaBr experiments, and yet the uptake is quite different. The data is pointing to a mechanism that is surface oriented, allows for negatively charged ions to approach a negatively charged surface, and that changes as a function of salt concentration and identity. Model development is currently underway to mathematically interpret the observed behaviors. In general, processes being considered are the effects of constrained interlayer space on water behaviors, and the formation of ion pairs either in the interlayer or as part of a surface complex. Within the fixed charge, nanostructured environment of clay minerals, water will orient as a function of charge. This orientation of water changes the dielectric properties, which in turn alters the effective hydration energies of ions. This change in dielectric properties favors more ion pair formation with increasing fixed surface charge. This conceptual model may explain the ability of iodide to concentrate in the interlayer. Instead of an anion, the iodide may be present as a neutral ion pair. Further, it may accumulate in the interlayer space as the ion pair formation is more favored in pore structures than it is in the bulk solution.

It cannot be stated with certainty, but it appears that the iodide remains as iodide and does not disproportionate to iodate for the studied conditions. IC analysis can separate these two ions. However, there is an unknown impurity in the clays that directly interferes with iodate quantitation. In desorption experiments, consisting of a four day DI water rinse after the end of an iodide batch experiment, iodide was present in the wash water. For certain clays (e.g., kaolinite) the impurity was present in smaller amounts. In these clays we may be able to say for certain whether disproportionation occurred. In clays with larger amounts of the impurity, this may remain uncertain. Further data analysis is underway to determine what can be definitively concluded about iodate in these systems.

## CONCLUSIONS/FUTURE WORK

In the literature, models describing clay protonation and sodium exchange are converging to a three site, four reaction model. One site and reaction is for  $\text{Na}^+/\text{H}^+$  exchange, one site and two reactions are devoted to the amphoteric protonation of Al-O edge sites, and the third site and final reaction is the protonation of the Si-O edge sites. The inversion method used here to interpret the titration curves gives consistent information between theory and experiment for the Al-O. However for the clays, the behaviors were far more disparate than expected. Comparing the results to the theory just described, the expectation would have been four distinct peaks; three would have been independent of ionic strength, and the fourth would have shifted consistently with ionic strength. Clearly this is not what occurred. It is unclear what is causing this discrepancy between published results and those presented here.

The iodide removals as a function of ionic strength and composition merit mathematical interpretations. If successfully described through a model incorporating ion pair formation, this will represent a significant shift in discourse regarding anion interactions with clays. While the presence of ion-pairing has been acknowledged in the literature [4], it has rarely been applied to data. The implications of this ion pair formation may inform the imperfect membrane effect observed in heavily compacted clay systems [5].

In the near future quantitative descriptions of the observed iodide uptake will be developed. This idea will be further tested under diffusive conditions in compacted clay columns. The characteristic length of pore structures in clay systems shifts downward with increasing compaction. The increased compaction increases the proportion of nano-scale environments analogous to that of the interlayer space in the clays. It is expected that as compaction increases, so would ion-pair formation, but the amount of ion-pair formation would also still be affected by the fixed charge in the interlayer space. The diffusion experiments will include a matrix of clays and compaction stresses to directly probe this idea.

## REFERENCES

1. Kahr, G. and F.T. Madsen, *Determination of the cation exchange capacity and the surface area of bentonite, illite and kaolinite by methylene blue adsorption*. Applied Clay Science, 1995. 9(5): p. 327-336.
2. Wang, Y.F., et al., *Control of pertechnetate sorption on activated carbon by surface functional groups*. Journal of Colloid and Interface Science, 2007. 305(2): p. 209-217.
3. Brady, P.V., R.T. Cygan, and K.L. Nagy, *Molecular Controls on Kaolinite Surface Charge*. Journal of Colloid and Interface Science, 1996. 183: p. 356-364.
4. Appelo, C.A.J., L.R. Van Loon, and P. Wersin, *Multicomponent diffusion of a suite of tracers (HTO, Cl, Br, I, Na, Sr, Cs) in a single sample of Opalinus Clay*. Geochimica Et Cosmochimica Acta, 2010. 74(4): p. 1201-1219.
5. Tournassat, C. and C.A.J. Appelo, *Modelling approaches for anion-exclusion in compacted Na-bentonite*. Geochimica Et Cosmochimica Acta, 2011. 75(13): p. 3698-3710.